$\alpha+{}^{12}$C inelastic angular distribution and nuclear size of ^{12}C(0_2^+)

M. Takashina[1,2,*] and Y. Sakuragi[2,3]

[1]*Yukawa Institute for Theoretical Physics, Kyoto University, Kyoto 606-8502, Japan*
[2]*RIKEN, Hirosawa 2-1, Wako, Saitama 351-0198, Japan*
[3]*Department of Physics, Osaka City University, Osaka 558-8585, Japan*

We analyze the inelastic scattering of α particles on ^{12}C exciting the 0_2^+ state at incident energies of $E_\alpha = 139$–240 MeV using α-condensate model wave functions, and investigate the effect of the nuclear radius of ^{12}C(0_2^+) on the inelastic angular distribution. It is found that the oscillation pattern in inelastic angular distribution is sensitive to the extension of the transition density rather than the nuclear radius of the excited state, although the absolute value of the inelastic differential cross section is sensitive to the nuclear radius of ^{12}C(0_2^+).

I. INTRODUCTION

The α-cluster correlation is known to be a fundamental feature of light nuclear systems, and the α-cluster structure of nuclei has been studied by many authors using various approaches [1]. A typical example is the three-α structure in ^{12}C, which has been studied using microscopic three-α-cluster models [2–5]. The results of these studies indicate that the 0_2^+ state in ^{12}C has a well-developed three-α-cluster structure, and the constituent α particles are moving freely as in a gas state.

Recently, it was proposed [6,7] that the 0_2^+ state in ^{12}C could be interpreted as an α-particle condensate state. The authors proposed a new type of α-cluster model describing an α-particle Bose-condensate state (α-condensate model, ACM). It was shown that this wave function reproduced well the experimental data on ^{12}C as well as the predictions of the microscopic three-α-cluster model by Kamimura *et al.* [3,4]. In that paper, it was also mentioned that ^{16}O probably had this kind of four-α-particle condensed state in the vicinity of the 4α threshold energy, and it was conjectured that such condensed α-cluster states might also occur in heavier $4n$ self-conjugate nuclei as excited states.

One of the remarkable features of the α condensed state is the dilute density distribution, resulting in a large nuclear radius of the state. Therefore, if the large nuclear radius of the candidate state is experimentally confirmed, it will be strong evidence of the formation of the α condensed state. However, the direct measurement of the nuclear radius or nucleon density distribution of excited states is not available at the moment. Therefore, an indirect procedure is necessary to prove the dilute density distribution of excited states. Very recently, Funaki *et al.* [8] analyzed the charge form factor of inelastic electron scattering to the 0_2^+ state of ^{12}C to discuss the spatial extension of this state using ACM. They studied the sensitivity of the form factor with respect to the nuclear size of the 0_2^+ state by varying the parameter β corresponding to the spatial extension of the α condensate. They found that only

the peak height of the form factor is sensitive to the size, while the positions of the peak and valley are almost unchanged. It was shown that the radius of excited states like the 0_2^+ state in ^{12}C could be deduced from the peak height of the inelastic charge form factor via their model wave function, although it is not a direct measurement of the nucleon density of the excited state.

Another idea for confirming the dilute density distribution of the 0_2^+ state was proposed by Ohkubo and Hirabayashi [9]. They analyzed the nuclear rainbow phenomenon in $\alpha+{}^{12}$C elastic and inelastic scattering angular distributions by the microscopic coupled-channels (MCC) approach. The calculation includes coupling to the 2_1^+ and 3_1^- states, which have normal shell-model-like density distributions, in addition to the ground and 0_2^+ states. Since they used the double-folding model interaction based on the resonating-group-method (RGM) wave function [4], the diluteness of the 0_2^+ state was properly taken into account. They showed that the volume integral of the folding-model potential in the $\alpha+{}^{12}$C(0_2^+) channel was much larger than those of $\alpha+{}^{12}$C(g.s., 2_1^+, 3_1^-) channels due to the density dependence of the effective interaction in the nuclear medium, and they argued that this large volume integral increased the number of minima in the Airy oscillation (Airy minima) in the angular distribution of the $\alpha+{}^{12}$C(0_2^+) channel: only one Airy minimum was observed in the angular distributions of elastic scattering and inelastic scattering to the 2_1^+ and 3_1^- states, while two Airy minima were observed in that of inelastic scattering to the 0_2^+ state. They concluded that the enhancement of Airy oscillation was evidence of the diluteness of the 0_2^+ density distribution.

To examine the effect of the diluteness of the 0_2^+ state on the angular distribution of inelastic scattering, it is important to investigate how the inelastic angular distribution is varied when the nuclear radius of the 0_2^+ state is changed. In the present study, we perform an MCC calculation for the $\alpha+{}^{12}$C inelastic scattering using the ACM wave functions obtained in Ref. [8], where the nuclear radius of the 0_2^+ state can be artificially changed, and investigate how the spatial extension of the 0_2^+ state is reflected in the details of the angular distribution of inelastic α scattering.

_____

*Electronic address: takasina@yukawa.kyoto-u.ac.jp

II. FORMALISM

We adopt the same formalism as that described in Ref. [9]: the MCC method based on the double-folding model using the DDM3Y interaction [10] for the effective nucleon-nucleon interaction. The density distribution of ^{12}C is given by the ACM calculations [7,8]. We refer to the ACM wave function originally obtained [7] as *original ACM*, and to those for which the spatial extension of the 0_2^+ state is artificially modified [8] as *modified ACM*. We use four types of modified ACM wave functions (i)–(iv), the root-mean-square (rms) radii $\langle r^2 \rangle^{1/2}$ of which are (i) 2.97 fm, (ii) 3.55 fm, (iii) 4.38 fm, and (iv) 5.65 fm, while that of the original ACM wave function is 3.81 fm [8]. It should be noted that the orthogonality of the 0_2^+ state and the 0_1^+ ground state wave functions is satisfied also in the modified ACM calculation. The transition density between the ground and 0_2^+ states is calculated from the ground state wave function and each of these wave functions for the 0_2^+ state. The ground state wave function is not modified throughout the present analysis.

The normalization factor N_R of the real folded potential and the parameters for the Woods-Saxon type imaginary potential are taken to be the same as those used in Ref. [9]. The volume integral per nucleon pair, J_v, and the rms radius $\langle R^2 \rangle^{1/2}$ of the folded potential for each ACM wave function at each incident energy are listed in Table I. The folded potentials of $\alpha + {}^{12}\mathrm{C}(0_2^+)$ for $E_\alpha = 240$ MeV with the DDM3Y interaction are shown in Fig. 1. The thick solid curve represents the folded potential using the original ACM wave function, while the other thick curves represent those with the modified ACM wave functions (i)–(iv). The folded potential of $\alpha + {}^{12}\mathrm{C}(\mathrm{g.s.})$ is also shown by the thin solid curve for comparison. All the folded potentials are multiplied by a common normalization factor N_R taken from Ref. [9]. It is found that as the nuclear radius of the 0_2^+ state increases, the potential at short distances becomes shallower. On the other hand, the potential around the surface region becomes stronger with the increase of the nuclear radius (due to the density dependence of the effective nucleon-nucleon interaction), which leads to the increase of the volume integral of the potential, as shown in Table I.

TABLE I. Volume integral per nucleon pair J_v and rms radius $\langle R^2 \rangle^{1/2}$ of the $\alpha + {}^{12}\mathrm{C}(0_2^+)$ diagonal folded potential calculated from the original and modified ACM wave functions and the DDM3Y interaction.

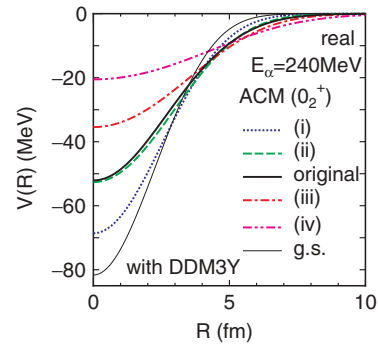| E_α (MeV)	Original	(i)	(ii)	(iii)	(iv)
	J_v (MeV fm^3)				
139.0	362	329	358	380	394
166.0	349	317	345	365	378
172.5	342	311	338	358	371
240.0	330	301	327	345	357
	$\langle R^2 \rangle^{1/2}$ (fm)				
139.0	4.60	3.92	4.36	5.05	6.18
166.0	4.60	3.92	4.37	5.05	6.18
172.5	4.61	3.93	4.37	5.06	6.18
240.0	4.62	3.95	4.39	5.07	6.19

FIG. 1. (Color online) Folded potential of $\alpha + {}^{12}\mathrm{C}(0_2^+)$ for $E_\alpha = 240$ MeV with the DDM3Y interaction. The thick solid curve represents the folded potential with the original ACM wave function, while the other thick curves represent those with the modified ACM wave functions (i)–(iv). The thin solid curve represents the folded potential of $\alpha + {}^{12}\mathrm{C}(\mathrm{g.s.})$. All the folded potentials are multiplied by the normalization factor from Ref. [9].

III. RESULTS AND DISCUSSIONS

Before showing the results of the MCC calculation using the ACM wave functions, we first perform an MCC calculation using the RGM wave functions [4] for ^{12}C, which were used in the previous MCC work [9], in order to confirm that our MCC calculation reproduces the results of Ref. [9]. Figures 2 and 3 show the angular distributions of $\alpha + {}^{12}$C elastic scattering and the inelastic one to the 0_2^+ state of ^{12}C at incident energies of $E_\alpha = 139$, 166, 172.5, and 240 MeV. In

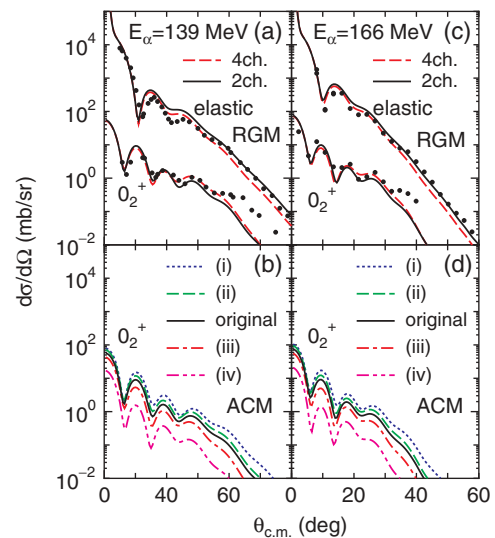FIG. 2. (Color online) Angular distributions of the elastic and $\alpha + {}^{12}\mathrm{C}(0_2^+)$ channels at the incident energies of $E_\alpha = 139$ and 166 MeV. In (a) and (c), dashed curves represent the result of the four-channel MCC calculation including the ground, 2_1^+, 3_1^-, and 0_2^+ states; solid curves represent the result of the two-channel calculation including the ground and 0_2^+ states. In both calculations, the DDM3Y interaction and the RGM wave function are used. Dots are the experimental data. In (b) and (d), the results are shown of the MCC calculations using the original ACM wave function (solid curve) and modified ACM wave functions (i)–(iv).
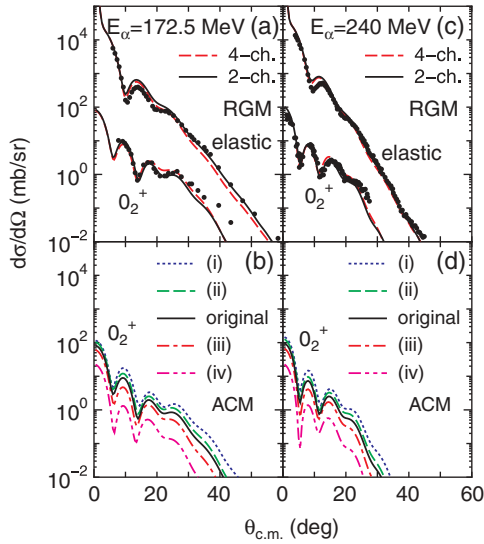
FIG. 3. (Color online) Same as Fig. 2, but for $E_\alpha = 172.5$ and 240 MeV.

FIG. 4. (Color online) Transition density between the ground state and the 0_2^+ one of ^{12}C calculated from the original and modified ACM wave functions (i)–(iv).

Figs. 2(a), 2(c) and Figs. 3(a), 3(c), the dots show experimental data [11–16], while the dashed curves are the results of four-channel MCC calculations including the ground, 2_1^+, 3_1^-, and 0_2^+ states of the ^{12}C nucleus where the RGM wave functions [4] are used to calculate the diagonal and coupling potentials. The calculations completely reproduce the results shown in Fig. 2 of Ref. [9]. The solid curves show the results of the two-channel MCC calculation in which only the ground and 0_2^+ states are included. It is seen that the effect of coupling to the 2_1^+ and 3_1^- states is almost negligible. Therefore, the two-channel calculation is enough to discuss the angular distribution of the $\alpha+{}^{12}$C(0_2^+) channel for these energies.

Next, we perform the two-channel MCC calculation using the original and modified ACM wave functions (i)–(iv) [7,8]. The result for the $\alpha+{}^{12}$C(0_2^+) channel is shown in Figs. 2(b), 2(d) and Figs. 3(b), 3(d). The solid curve in each figure represents the result with the original ACM wave function used. Since the original ACM wave function is almost equivalent to the RGM one as shown in Ref. [7], the solid curves in Figs. 2(b), 2(d) and Figs. 3(b), 3(d) are almost the same as those in Figs. 2(a), 2(c) and Figs. 3(a), 3(c), respectively. The other curves are the results of two-channel MCC calculations in which the modified ACM wave functions (i)–(iv) are used, where we use the same Woods-Saxon type imaginary potential as that used in the calculations for the solid curves. It is found that the oscillation pattern of the angular distribution is hardly changed for any of the incident energies even when the density distribution of the 0_2^+ state is artificially shrunk or extended, although the absolute value changes. This is because the change of the nuclear radius of the excited 0_2^+ state has little effect on the shape of the transition density between the ground state and the 0_2^+ one; it only changes the magnitude of the transition density, as shown in Fig. 4.

We also perform the same coupled-channel calculation for $E_\alpha = 240$ MeV using another interaction model. We adopt the single-folding model based on the nucleon-α interaction,
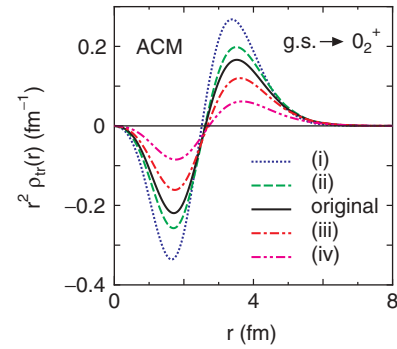
in which an empirical nucleon-α complex potential [17] is folded with the nucleon density of ^{12}C leading to a complex α-^{12}C potential. The nucleon-α potential parameters are taken from Ref. [17] except for the strength of the imaginary part W, which is set to 8.0 MeV in the present work so as to reproduce the α-^{12}C elastic scattering angular distribution. The real part of the diagonal and coupling potentials calculated in this single-folding model are found to be almost identical to those calculated in the double-folding model with the DDM3Y interaction. Using the single-folding interaction, we obtain the imaginary potential as well as the real one, and the shape of the imaginary potential also reflects the difference in the density distribution of the 0_2^+ excited state through the folding procedure. The result using the original ACM wave function is shown in Fig. 5(a). It is found that the angular distribution of the $\alpha+{}^{12}$C(0_2^+) channel is well reproduced. The results for the modified ACM wave functions (i)–(iv) are shown in Fig. 5(b). The solid curve is the same as that in Fig. 5(a) for the 0_2^+ state. The obtained results are very similar to the previous calculation shown in Figs. 2 and 3 where the DDM3Y real folding interaction and a fixed Woods-Saxon type imaginary potential were used. The result implies that the qualitative conclusion drawn from the results seen in Figs. 2 and 3 is not
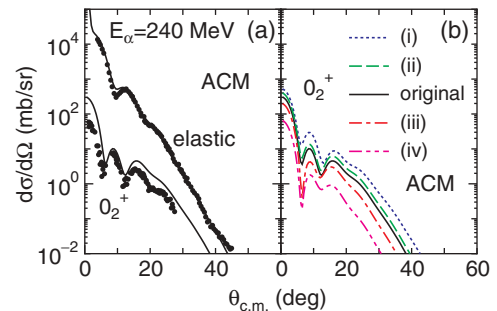

FIG. 5. (Color online) Angular distribution of the elastic and $\alpha+{}^{12}$C(0_2^+) channels at the incident energy of $E_\alpha = 240$ MeV. (a) Solid curves are the result of the MCC calculation using the nucleon-α single-folding model interaction. Dots are experimental data. (b) Solid curve is the same as in (a); other curves show results of the MCC calculations with the modified ACM wave functions (i)–(iv).
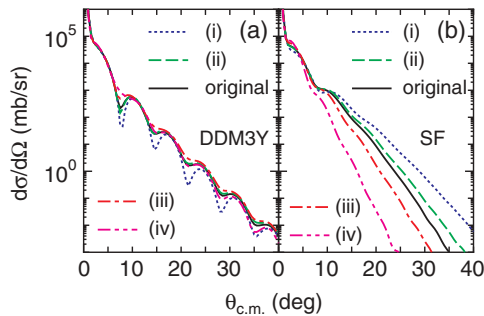
FIG. 6. (Color online) Angular distribution of $\alpha + {}^{12}C(0_2^+)$ elastic scattering at $E_\alpha = 240$ MeV, obtained with original (solid curves) and modified (other curves) ACM wave functions. (a) DDM3Y interaction and (b) nucleon-α single-folding interaction.

FIG. 8. (Color online) Angular distribution of $\alpha + {}^{12}C(0_2^+)$ channel at $E_\alpha = 240$ MeV, obtained with the original ACM wave function and with the modified transition densities as in Eq. (1). (a) DDM3Y interaction case. (b) Nucleon-α single-folding model interaction case.

affected by the change of the imaginary potentials due to the change of the spatial extension of the 0_2^+ state.

To see the distortion effect of the final channel, we perform the single-channel calculation, where $\alpha + {}^{12}C(0_2^+)$ is virtually set to the incident channel (Fig. 6). For the DDM3Y case, shown in Fig. 6(a), it is found that the minimum positions are not shifted even when the nuclear radius of ${}^{12}C(0_2^+)$ becomes large. This is because the parameters of the imaginary potential are the same in all calculations. Figure 6(b) shows the result where the nucleon-α single-folding model interaction is used. Although the oscillation in the backward angle region is found to be smeared, the variation of the elastic angular distributions due to the modification of nuclear radius of ${}^{12}C(0_2^+)$ is clearly seen. Nevertheless, this variation seems not to be inherited by the inelastic scattering case as shown in Fig. 5(b). This result indicates that the inelastic angular distribution is insensitive to the distortion effects in the final channel.

From the results above, we can say that the number of minima and the minimum positions in the inelastic angular distribution are almost unchanged by the modification of the nuclear radius of the 0_2^+ state. This result may be due to the nature of the transition density: the nodal position and the point where the transition density drops approximately to zero do not depend on the nuclear radius of the 0_2^+ state as shown in Fig. 4. In other words, the transition density does not

sensitively reflect the size of the 0_2^+ state. To investigate the sensitivity of the inelastic angular distribution to the extension of the transition density, we perform MCC calculations using a transition density, whose range is artificially modified as

$$\rho'_{tr}(r) = N\rho_{tr}(fr), \qquad (1)$$

where $\rho_{tr}(r)$ is the original ACM transition density, and f and N are scaling and normalization factors, respectively. N is determined so as to keep the r^2 moment of the transition density to the value evaluated from the original transition density. The modified transition densities are shown in Fig. 7 along with the original one (solid curve). Using these transition densities, we perform MCC calculations in which we fix the diagonal density of 0_2^+ state to the original one. The results of the calculations are shown in Fig. 8. The differential cross sections in Fig. 8(a) are calculated with DDM3Y double-folding model interaction, while those in Fig. 8(b) are calculated with the nucleon-α single-folding model interaction. In both cases, the minimum positions in the angular distribution are very sensitive to the range of the transition density. Inversely, the extension of the transition density can be probed by the the shape of the oscillation in the inelastic angular distribution.

IV. CONCLUSION

In the present paper, we conclude that one can determine the extension of the transition density from the oscillation pattern of the inelastic angular distribution rather than the nuclear radius of the excited state. However, the nuclear radius of the excited state can be deduced from the absolute value of the inelastic differential cross sections through the amplitude of the transition density calculated in a microscopic nuclear structure model such as ACM, as shown in Ref. [8]. Therefore, it is very interesting to analyze the α-particle inelastic scattering on ${}^{16}O$ exciting the 0^+ state at $E_x = 13.5$ MeV, recently measured [18], by the MCC calculation using the wave function of ${}^{16}O(0^+)$ obtained by the ACM calculation at $E_x = 14.1$ MeV [8], which is predicted as a four-α condensed state.
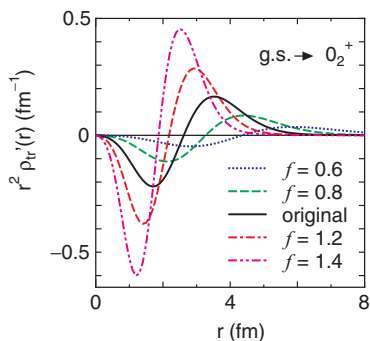

FIG. 7. (Color online) Transition density modified by Eq. (1), where the scaling factor f is varied from 0.6 to 1.4. Modified transition densities are normalized to keep the r^2 expectation value evaluated from the original transition density (solid curve).
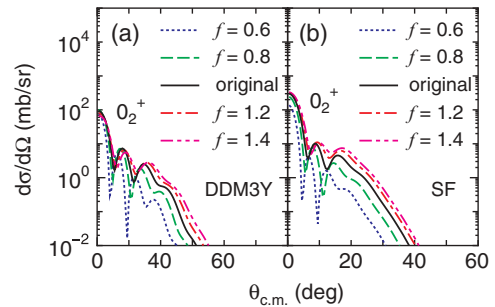
[1] For example, Y. Fujiwara, H. Horiuchi, K. Ikeda, M. Kamimura, K. Kato, Y. Suzuki, and E. Uegaki, Prog. Theor. Phys. Suppl. **68**, 29 (1980).

[2] H. Horiuchi, Prog. Theor. Phys. **51**, 1266 (1974); **53**, 447 (1975).

[3] Y. Fukushima and M. Kamimura, J. Phys. Soc. Jpn **44**, 225 (1978).

[4] M. Kamimura, Nucl. Phys. **A351**, 456 (1981).

[5] E. Uegaki, S. Okabe, Y. Abe, and H. Tanaka, Prog. Theor. Phys. **57**, 1262 (1977); E. Uegaki, Y. Abe, S. Okabe, and H. Tanaka, *ibid.* **62**, 1621 (1979).

[6] A. Tohsaki, H. Horiuchi, P. Schuck, and G. Röpke, Phys. Rev. Lett. **87**, 192501 (2001).

[7] Y. Funaki, A. Tohsaki, H. Horiuchi, P. Schuck, and G. Röpke, Phys. Rev. C **67**, 051306(R) (2003).

[8] Y. Funaki, A. Tohsaki, H. Horiuchi, P. Schuck, and G. Röpke, Eur. Phys. J. A **28**, 259 (2006); Y. Funaki (private communication).

[9] S. Ohkubo and Y. Hirabayashi, Phys. Rev. C **70**, 041602(R) (2004).

[10] M. El-Azab Farid and G. R. Satchler, Nucl. Phys. **A438**, 525 (1985).

[11] S. M. Smith *et al.*, Nucl. Phys. **A207**, 273 (1973).

[12] I. Brissaud *et al.*, Phys. Lett. **B30**, 324 (1969).

[13] S. Wiktor *et al.*, Acta Phys. Pol. B **12**, 491 (1981).

[14] A. Kiss *et al.*, J. Phys. G **13**, 1067 (1987).

[15] B. John, Y. Tokimoto, Y. W. Lui., H. L. Clark X. Chen, and D. H. Youngblood, Phys. Rev. C **68**, 014305 (2003).

[16] The experimental data of Refs. [11–15] are retrieved from EXFOR at IAEA-NDS (International Atomic Energy Agency-Nuclear Data Service, web site http://www-nds.iaea.org/

[17] A. Kolomiets, O. Pochivalov, and S. Shlomo, Phys. Rev. C **61**, 034312 (2000).

[18] T. Wakasa (private communication).